3D Finite Element analysis of stud anchors with large head and embedment depth

G. Periškić, J. Ožbolt & R. Eligehausen
Institute for Construction Materials, University of Stuttgart, Stuttgart, Germany

ABSTRACT: In the present paper results of the finite element study for headed stud anchors loaded in tension (concrete cone failure) are presented and discussed. The numerical analysis was performed using a 3D FE code based on the microplane model. Considered are anchors with extremely large embedment depths (up to 1143 mm). For each embedment depth the size of the head of the anchor was varied in order to account for the influence of pressures under the anchor head. Furthermore, for the anchor group of four anchors, the influence of the head size on the characteristic spacing of anchors was investigated. The results of the finite element study are discussed and compared with the recently performed test results and with current code recommendations.

1 INTRODUCTION

In engineering practice headed anchors are often used to transfer loads into reinforced concrete. Experience and large number of experiments and numerical studies with anchors of different sizes, confirmed that fastenings are capable of transferring tension forces into a concrete member without the need for reinforcement (Eligehausen et al. 2006). Provided that the strength of anchor steel and the load bearing area of anchor head are large enough, a headed stud subjected to tensile load normally fails by a cone shaped concrete breakout.

To better understand the crack growth and to predict the concrete cone failure load of headed studs for different embedment depths, a number of experimental and theoretical studies have been carried out (Eligehausen et al. 2006). Due to the fact that the tests with large embedment depths require massive test equipment, most of the experiments were up to now performed with embedment depths in the range from h_{ef} = 100 to 500 mm. Furthermore, in the tests the size of the headed studs is usually chosen such that the compressive stress under the head at peak load is approximately 20 times larger than the uniaxial compressive strength of concrete (f_c). However, in engineering practice, especially in nuclear power plants, anchors with larger embedment depths and with larger head sizes relative to the embedment depth are frequently used. These anchors are designed according to the current design code recommendations, which are based on the experimental results obtained for fasteners with relatively small embedment depths and head sizes. Therefore, to investigate the safety of these anchors, additional experiments are needed. Since these experiments are extremely expensive, failure capacity of large anchors can alternatively be obtained by numerical analysis.

In the last two decades significant work has been done in the development and further improvement of numerical tools. These tools can be employed in the analysis of non-standard anchorages. Unfortunately, the objectivity of the numerical simulation depends strongly on the choice of the material model. Therefore, the numerical results should be confirmed by experiments and the numerical model used should pass some basic benchmark tests. In the present paper the three-dimensional finite element analysis is carried out using the finite element (FE) code MASA. The code is based on the microplane model for concrete. On a very large number of numerical examples that have been carried out in the past, it has been demonstrated that the code is able to predict failure of concrete and reinforced concrete structures realistically (Ožbolt 2001).

2 FINITE ELEMENT CODE

The FE code employed in the present study is aimed to be used for the two- and three-dimensional nonlinear analysis of structures made of quasi-brittle materials such as concrete. It is based on the microplane material model (Ožbolt et al. 2001) and smeared crack approach. To avoid mesh dependent

sensitivity, either the crack band approach (Bažant & Oh 1983) or the nonlocal integral approach (Ožbolt & Bažant 1996, Pijaudier-Cabot & Bažant 1987) can be employed. The spatial discretization of concrete is performed using four or eight node solid finite elements. The reinforcement can be modelled by discrete bar elements with or without discrete bond elements or, alternatively, smeared within the concrete elements. The analysis is carried out incrementally, i.e. the load or displacement is applied in several steps. The preparation of the input data (pre-processing) and evaluation of numerical results (post-processing) are performed using the commercial program FEMAP®.

In the microplane model, material properties are characterized on planes of various orientations at a finite element integration point. On these microplanes there are only a few uniaxial stress and strain components and no tensorial invariance requirements need to be considered. The tensorial invariance restrictions are satisfied automatically since microplanes simulate the response on various weak planes in the material (inter-particle contact planes, interfaces, planes of microcracks, etc.). The constitutive properties are entirely characterized by relations between normal and shear stress and strain components on each microplane. It is assumed that the strain components on microplanes are projections of the macroscopic strain tensor (kinematic constraint approach). Knowing the stress-strain relationship of all microplane components, the macroscopic stiffness and the stress tensor are calculated from the actual strains on microplanes by integrating of stress components on microplanes over all directions. The simplicity of the model lies in the fact that only uniaxial stress-strain relationships are required for each microplane component and the macroscopic response is obtained automatically by integration over all microplanes. For more details see Ožbolt et al. (2001).

Due to the loss of elipticity of the governing differential equations, the classical local smeared fracture analysis of materials, which exhibit softening (quasi-brittle materials), leads in the finite element analysis to results, which are in general mesh dependent. To assure mesh independent results the total energy consumption capacity due to cracking must be independent of the element size, i.e. one has to regularize the problem by introducing the so-called localization limiter. In the present numerical study the crack band approach (Bažant & Oh 1983) is used. In this approach the constitutive law is related to the element size such that the specific energy consumption capacity of concrete (concrete fracture energy G_F) is independent of the size of the finite element.

3 NUMERICAL ANALYSIS – RESULTS AND DISCUSSION

The main purpose of the 3D FE analysis was to investigate the ultimate capacity and failure mode for single anchors with extremely large embedment depths and with two different head sizes, which are pulled-out from a concrete block. Moreover, the influence of the head size on the critical anchor spacing for group of four anchors, obtained by Rah (2005) is also discussed.

3.1 *Single anchor*

The typical geometry of the concrete block and the geometry of the headed stud are shown in Figure 1. Three embedment depths were numerically investigated, namely h_{ef} = 635, 889 and 1143 mm. For each embedment depth two head sizes were used (small and large). The geometrical properties for all investigated cases are summarized in Table 1.

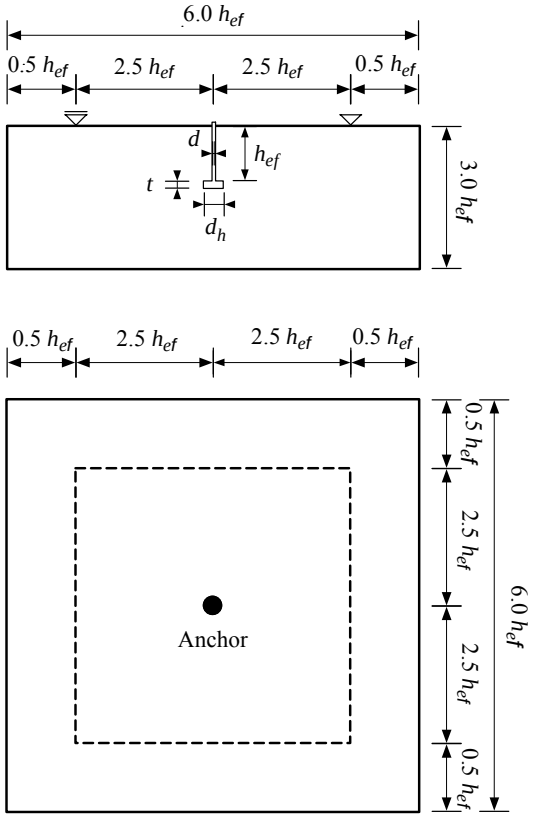

Figure 1. Geometry used in the pull-out study.

Table 1. Geometric properties.

h_{ef}	d	t	$d_{h,small}$	$d_{h,large}$
635	70	76	83	118
889	95.3	102	105	162
1143	160.8	169	171	241

The size of the smallest head for all embedment depths is chosen such that the compressive stress

under the head at peak load is 20 times larger than the uniaxial cylindrical compressive strength of concrete (f_c). The peak load is calculated based on the concrete cone capacity method (Eligehausen et al. 2006). The large sizes are chosen to be typical for engineering practice (nuclear power plants). The concrete properties are taken as: Young's modulus $E_c = 28000$ MPa, Poisson's ratio $\nu_c = 0.18$, tensile strength $f_t = 3.0$ MPa, uniaxial compressive strength $f_c = 38$ MPa and concrete fracture energy $G_F = 0.10$ N/mm. The behaviour of steel is assumed to be linear elastic with Young's modulus $E_s = 200000$ MPa and Poisson's ratio $\nu_s = 0.33$.

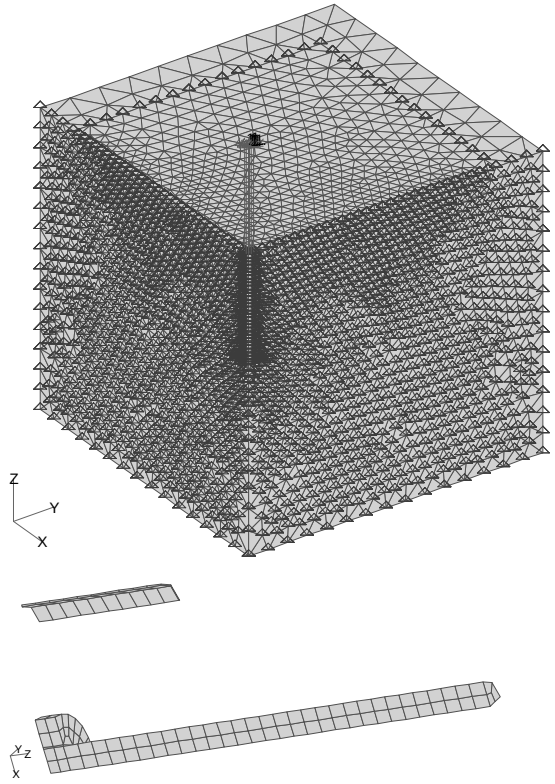

Figure 2. Typical FE meshes of concrete block and headed stud with contact elements.

Spatial discretization is performed using four node solid finite elements. Only one quarter of the concrete block is modelled, i.e. double symmetry is utilized. Typical finite element meshes of the concrete block and headed stud are shown in Figure 2. Contact between the steel stud and concrete exists only on the top of the headed stud (compression transfer zone). To account for the confining stresses that develop in the vicinity of the head, interface elements, which can take up only compressive stresses are used (see Fig. 2). In all cases the anchor is loaded by prescribed displacements at the top of the anchor shaft. The supports were fixed in the vertical (loading) direction. The distance between the support and the anchor is taken as $2.5h_{ef}$ so that an unrestricted formation of the failure cone is possible (see Fig. 1).

Typical load-displacement curves for two different head sizes ($h_{ef} = 635$ mm) are shown in Figure 3. The curves show that anchors with small heads have larger displacements at peak load. According to the FE analysis this tendency is stronger if the embedment depth is larger.

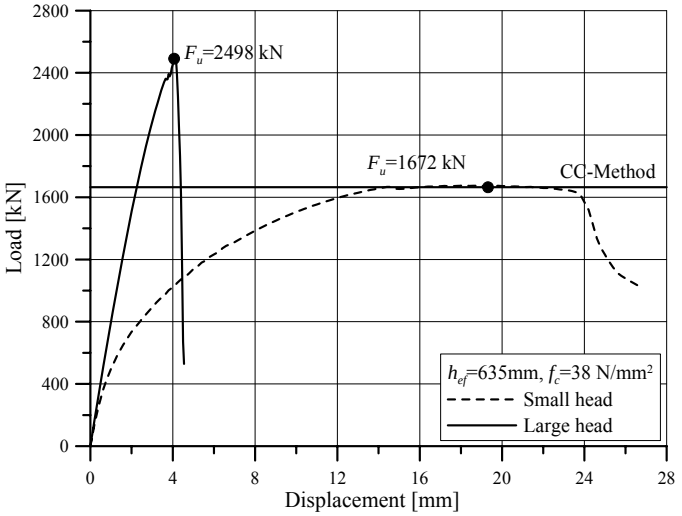

Figure 3. Typical load-displacement curves for two different head sizes ($h_{ef} = 635$ mm).

The summary of the predicted peak loads (F_u) from the FE simulation as well as the available experimental results is given in Table 2. In the same table the peak loads according to Equation 1, which is the base of ETAG CC design code (Eligehausen et al. 2006):

$$F_u = 15.5\sqrt{f_{cc}}\,h_{ef}^{1.5} \tag{1}$$

and according to Equation 2, which is the base of ACI-349-01 design code (ACI Standard 349 2001):

$$F_u = \alpha\sqrt{f_c}\,h_{ef}^{\beta}$$

$$0 < h_{ef} < 279.4;\ \alpha = 16.834;\ \beta = 1.5 \tag{2a}$$

$$279.4 \le h_{ef} \le 635;\ \alpha = 6.585;\ \beta = 5/3 \tag{2b}$$

are displayed. In Equation 1 $f_{cc} = 1.2\ f_c$.

Table 2. Predicted peak loads.

h_{ef} [mm]	F_u [kN] Eq. 1	Eq.2	FE ($d_{h,small}$)	FE ($d_{h,large}$)	Test ($d_{h,large}$)
635	1664	1946	1675	2498	2250
889	2756	3413	2707	3806	3300
1143	4018	5193	4076	5780	5500

It should be noted that Equation 1 was calibrated using experiments in which the maximum embedment depth was 500 mm and the head size small, as defined above. Moreover, the exponent 1.5 (see Eq. 1)

indicates the size effect on the concrete cone failure resistance according to linear elastic fracture mechanics (LEFM), i.e. maximum possible size effect.

Numerically obtained peak loads for anchors with small head sizes show very good agreement with Equation 1 (max difference less than 2%). However, for anchors with large heads the difference between numerical results and Equation 1 is obvious (see Table 2). Furthermore, in the tests recently performed in Korea (Lee et al. 2006), where the size of the anchor head was very similar to large heads in the present FE study, measured ultimate loads are significantly higher than according to Equation 1. These ultimate loads agree better with Equation 2, i.e. the largest difference is 15% for $h_{ef} = 635$ mm and it tends to be smaller with increase of the embedment depth (6% for $h_{ef} = 1143$ mm). The test results (Lee et al. 2006) and FE results for large heads show good agreement, however, the absolute values of peak loads measured in experiments somewhat underestimate the numerical results obtained for anchors with large heads (up to 15%). There could be different reasons for this. For instance, the tests were performed on huge specimens with boundary conditions, which were possibly not the same as assumed in the analysis. Furthermore, the concrete mechanical properties adopted in the analysis were the same as the concrete properties measured on the laboratory specimen. However, the mechanical properties of test specimen (strength and fracture energy) were possibly reduced due to the effect of non-elastic deformations (shrinkage, temperature, etc.). These effects were not accounted for in the analysis. Nevertheless, the test results confirm the numerical results, which clearly show that with increase of the anchor head size the anchor resistance increases.

The typical calculated crack patterns for two different head sizes ($h_{ef} = 635$ mm) are shown in Figure 4. The cracks (dark zones) are plotted by means of maximum principal strain. A critical crack opening $w_{cr} = 0.2$ mm is assumed. This crack opening corresponds to the plotted critical principal strain of $\varepsilon_{cr} = w_{cr}/h_E$, where h_E = average element size. The crack patterns are shown for the post-peak anchor resistance. It was observed that for smaller anchor heads the crack length at peak load is shorter than the crack length obtained for the anchors with larger anchor heads. Moreover, the crack propagation angle, measured from the loading direction, increases with increase of head size. For small head sizes, the concrete cone is steeper than in the case of large head sizes (see Fig. 4). This tendency of having a flatter concrete cone in case of large head sizes was also confirmed in the tests (Lee et al. 2006), where the angle between the failure surface of the concrete cone and concrete surface varied from 20° to 30°. According to ETAG-CC method, this angle is assumed to be approximately 35° and it agrees well with the numerical results obtained for anchors with small heads (see Fig. 4a).

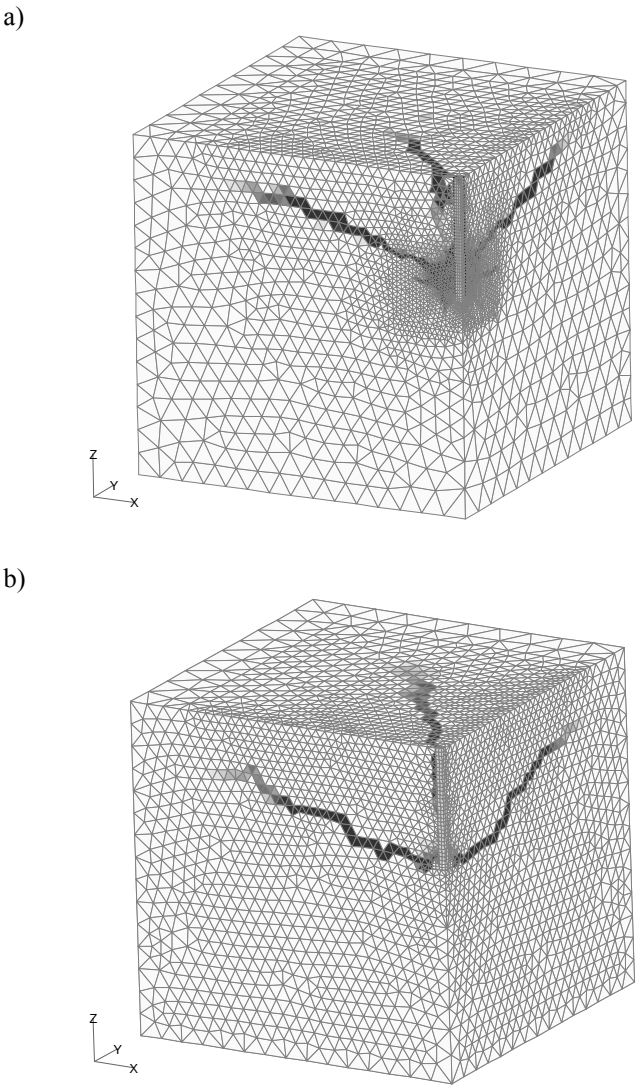

Figure 4. Typical crack patterns: a) small head, $h_{ef} = 635$ mm and b) large head, $h_{ef} = 635$ mm.

The numerical results confirm that there is a strong size effect on the concrete cone resistance. In Figure 5 the calculated relative failure resistance ($\sigma_R = \sigma_N/\sigma_{N,hef=200}$, with $\sigma_N = F_u/(h_{ef}^2 \pi)$) is plotted as a function of the embedment depth. Since no FE calculation was carried out for $h_{ef} = 200$ mm, a predicted ultimate load according to Equation 1 was taken as a reference value. For comparison, the prediction according to Equation 1 is also plotted. Note that the size effect is strong if the gradient of the relative resistance with respect to the embedment depth ($\partial\sigma_R/\partial h_{ef}$) is large. As mentioned before, Equation 1 predicts the maximum size effect (LEFM). From Figure 5 it can be seen that the numerical results for anchors with small anchor heads agree well with Equation 1, i.e. they predict strong size effect. However, with increase of the anchor head size the size effect on the relative anchor resistance decreases. The reason why the predicted size

effect agrees well with the size effect prediction according to LEFM for fasteners with small heads is due to the fact that for all embedment depths the crack patterns and the crack length at peak load are geometrically similar, i.e. the crack length is relatively small and approximately proportional to the embedment depth. The main assumption of LEFM, namely the proportionality of the crack length at peak load, is fulfilled and therefore the size effect follows the prediction according to LEFM. On the contrary, for fasteners with larger heads the crack pattern at peak load is not proportional when the embedment depth increases. This is the case for both, the crack length at peak load and for the corresponding shape of the failure cone. Consequently, the size effect on the concrete cone failure load is smaller.

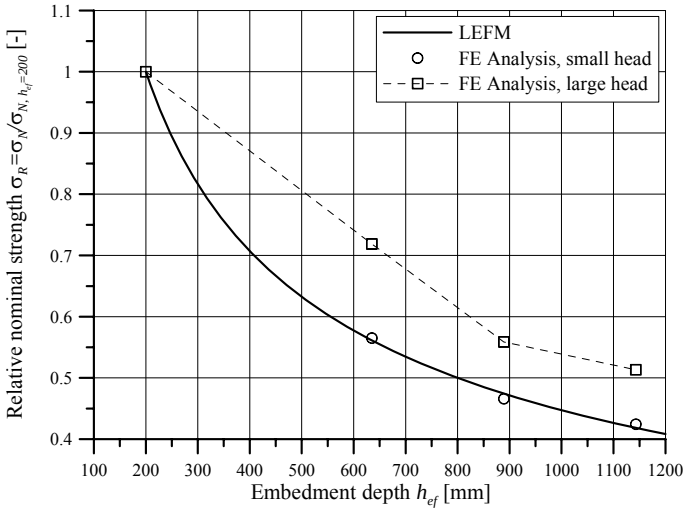

Figure 5. Relative concrete cone resistance as a function of the embedment depth.

The fact that the concrete cone resistance increases with increase of the head size of the anchor is closely related to local pressure under the head of the stud. This has already been reported by Furche (1994) (see Fig. 6). When the head of the anchor is small, the pressure under the head is relative to fc high and the concrete under the head is significantly damaged. In the vicinity of the head, rather complex mixed-mode fracture (compression-shear) takes place and the displacement of the anchor in load direction increases due to shearing. This leads to a reduction of the effective embedment depth and causes the formation of a relatively steep concrete cone (see Fig. 6). However, in the case of anchors with large heads the concrete under the head is practically undamaged because of relatively small pressure and the crack starts to propagate in mode-I failure mode almost horizontally (see Figs. 4 and 6). Consequently, a larger cone surface forms which provide higher concrete-cone pull-out resistance.

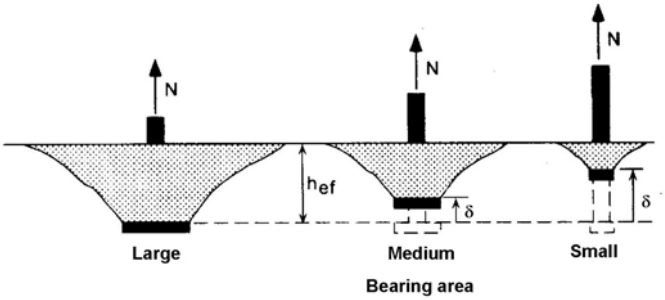

Figure 6. Concrete breakout cones of headed studs with heads of various diameters (schematic) according to Furche (1994).

Figure 7 shows the relation between failure load, calculated and in the experiment measured, and the failure load according to Equation 1 as a function of pressure under the anchor head at ultimate load. The pressure under the anchor head p is calculated as

$$p = \frac{F_u}{A_{ef}\, f_c} \tag{3}$$

in which A_{ef} = the load bearing area of the anchor. The results of the FE analysis for both head sizes and test results according to experimental tests from Korea (Lee et al. 2006) are shown. Furthermore, the results of the FE analysis obtained recently by Rah (2005) are also shown. It can be seen, that the numerically and experimentally obtained failure loads increase with decreasing pressures under the head i.e. with increasing head size.

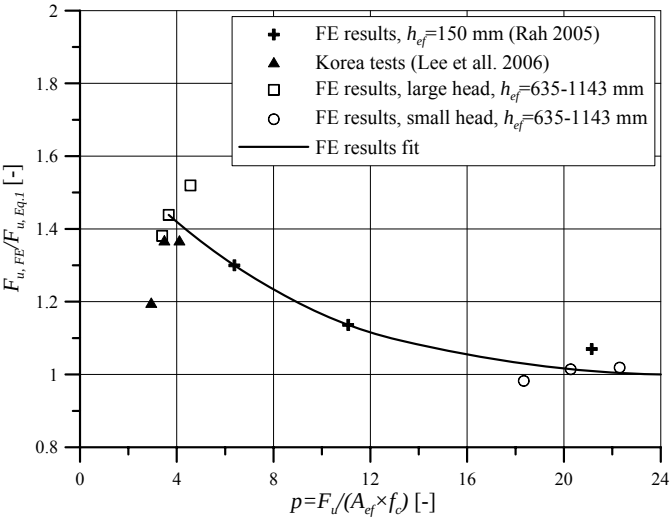

Figure 7. Relative ultimate capacity of headed studs as a function of pressures under the anchor head at peak load.

As it can be seen from Figure 7, if the pressures under the anchor head are relatively large ($p = 20 f_c$) the ultimate load agrees very well with the prediction according to Equation 1. According to the recent test results (Lee et al. 2006), as the pressure decreases the ultimate load increases and reaches about 140%

($p = 4f_c$) of failure load predicted by Equation 1. This shows that the Equation 1 is conservative in case of anchors with small pressure under the anchor head at peak load.

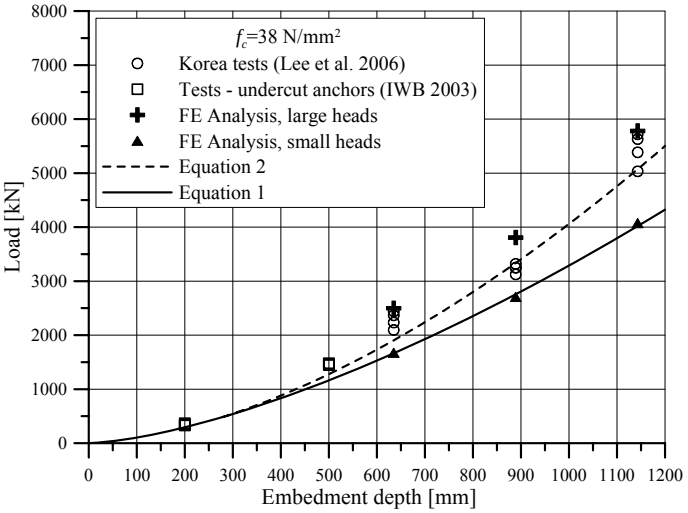

Figure 8. Ultimate load versus embedment depth comparison between calculated data, test data and design formulas.

All results are summarized in Figure 8 in form of ultimate loads as a function of embedment depth. Note that Figure 8 also shows recent results obtained for undercut anchors with embedment depths of 200 and 500 mm (IWB 2003). The figure shows that for embedment depths up to 300 mm, test results agree well with both design codes. However, for larger embedment depths and for anchors with large head sizes the ultimate load predicted by Equation 1 is too conservative. As shown before, the anchors with large heads exhibit smaller size effect on the ultimate load than the anchors with smaller heads. Therefore, their load bearing capacity is better predicted by Equation 2, which accounts for the size effect that is weaker the prediction according to LEFM.

As already mentioned, and also discussed recently (Ozbolt et al. 2004) the pressures under the anchor head at peak load could be used to control the influence of the anchor head size on the ultimate anchor load. Principally, for relatively high pressure the Equation 1 can be used. However, for larger embedment ($h_{ef} > 300$ mm) and larger head sizes the prediction according to Equation 2 seems to be more appropriate.

3.2 *Group of anchors*

A possible problem in using current design codes for anchors with large embedment depths and with large heads could be the safety of anchor groups. As mentioned before, concrete cone propagates somewhat flatter in case of anchors with large heads than in the case of anchors with small heads. In recent tests the concrete cone propagation angle between concrete surface and cone surface varied from 20–30° (Lee et al. 2006). This would imply that the characteristic spacing of anchors $s_{cr,N}$ for group of anchors could be larger than currently proposed by both design codes, i.e. $s_{cr,N} = 3h_{ef}$.

Figure 9 shows the results of FE analysis recently obtained by Rah (2005). The influence of anchor spacing s on the ultimate bearing capacity of groups of 4-anchors for large anchor heads was investigated. In the same figure the Equation 4:

$$F_u^G = F_u \cdot \frac{A_N}{A_N^o} \tag{4}$$

F_u^G = Ultimate load for group of 4 anchors

F_u = Ultimate load of single anchor (Eq. 1 or Eq. 2)

$A_N^o = 9h_{ef}^2$

$A_N = (3h_{ef} + s)^2; \quad s \le s_{cr,N} = 3h_{ef}$

which is the base of ETAG-CC and ACI-349-01 for predicting of ultimate load for groups of 4 anchors is plotted as well. As can be seen from Figure 9, the predicted average characteristic anchor spacing is approximately $5h_{ef}$. This means that the interaction between the anchors of the group exists for larger spacing range than according to Equation 4. Therefore, to clarify this question further numerical and experimental investigations are needed.

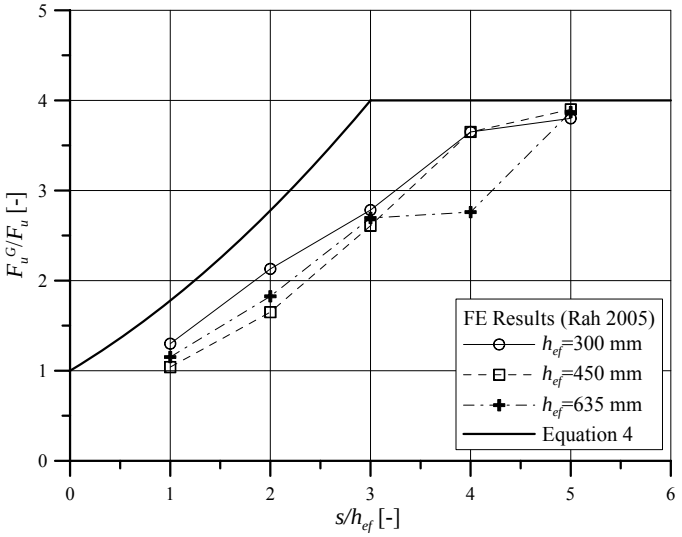

Figure 9. Relative ultimate load of 4-anchor groups as a function of anchor spacing s divided with embedment depth h_{ef} – FE results according to Rah (2005) and ultimate load prediction according to Equation 4.

4 CONCLUSIONS

In the present paper the behavior of large anchor bolts embedded in concrete is numerically investigated. The numerical results are compared with available test data and current design recommenda-

tions. Based on the results, the following can be concluded: (1) The concrete cone capacities predicted by the FE analysis for anchors with small heads show for the entire investigated range of embedment depths good agreement with Equation 1, which is the based on LEFM. However, for anchors with larger heads the numerical results indicate higher resistance than predicted by Equation 1; (2) The numerical study confirms the strong size effect on the concrete cone resistance. By increasing the head size of the stud, the size effect on the failure capacity of anchors decreases; (3) The available test data for anchors with larger heads confirm the tendency observed in the numerical study, i.e. the concrete cone resistance increases with increase of the head size; (4) The influence of the size of the anchor head on the ultimate load can be suitably described using pressures under the anchor head at peak load; (5) For pressures larger than approximately $4f_c$ Equation 1 predicts realistic results. For $p < 4f_c$ Equation 1 underestimates the resistance and more realistic prediction is given by Equation 2; (6) For group of anchors with larger head sizes, the characteristic anchor spacing seem to be larger than the code prediction ($3h_{ef}$). Therefore, to improve and to extend the validity of the current design recommendations, further theoretical, experimental and numerical investigation is needed.

REFERENCES

ACI Standard 349-01/349R-01 2001. *Code Requirements for Nuclear Safety Related Concrete Structures and Commentary (ACI 349R-01).*

Bažant, Z.P. & Oh, B.-H. 1983. Crack Band Theory for Fracture of Concrete. *Materials and Structures* 93(16): 155-177.

Eligehausen, R., Mallée, R. & Silva, J.F. 2006. *Anchorage in Concrete Construction.* Ernst & Sohn, Berlin, Germany.

Furche, J. 1994. *Load-bearing and displacement behaviour of headed anchors under axial tension loading.* Doctor thesis, Institute for construction materials, University of Stuttgart, Germany.

IWB 2003. *Ausziehversuche mit dem Hochtief Schwerlastanker HT-SHV in Beton.* Internal report of the Institute for construction materials, University of Stuttgart, Germany.

Lee, N.H., Kim, K.S., Bang, C.J. & Park, K.R. 2006. Tensile anchors with large diameter and embedment depth in concrete. *Submitted to ACI Stuctural and Materials Journals*.

Ožbolt, J. & Bažant, Z.P. 1996. Numerical smeared fracture analysis: Nonlocal microcrack interaction approach. *International Journal for Numerical Methods in Engineering* 39(4): 635-661.

Ožbolt, J., Li, Y.-J. & Kožar, I. 2001. Microplane model for concrete with relaxed kinematic constraint. *International Journal of Solids and Structures* 38: 2683-2711.

Ožbolt, J. 2001. Smeared fracture finite element analysis – Theory and examples. In Rolf Eligehausen (ed.), *International symposium on Connections between Steel and Concrete,* RILEM, SARL: 609-624.

Ožbolt, J., Periškić, G., Eligehausen, R. & Mayer, U. 2004. 3D FE Analysis of anchor bolts with large embedment depths. *Fracture mechanics of concrete structures; Proc. 5. intern. conf. on fract. mech. of conc. struct.,* Vail, Colorado, USA: 845-853.

Pijaudier-Cabot, G. & Bažant, Z.P. 1987. Nonlocal Damage Theory. *Journal of Engineering Mechanics* 113(10): 1512-1533.

Rah, K.K. 2005. *Numerical study of the pull-out behaviour of headed anchors in different materials under static and dynamic loading conditions.* Master thesis, Institute for Construction materials, University of Stuttgart, Germany.